

# Iterative Space Transformation Enables the Use of Optimal Magnetic Field Correction Algorithms Using EPI-based Field Maps

A. Hahn<sup>1</sup>, A. Nencka<sup>1</sup>, and D. Rowe<sup>2</sup>

<sup>1</sup>Biophysics, Medical College of Wisconsin, Milwaukee, WI, United States, <sup>2</sup>Mathematics, Statistics, and Computer Science, Marquette University, Milwaukee, WI

**Introduction:** Estimations of the inhomogeneities in the main magnetic field in MRI can be used to correct errors such as warping and intensity artifacts in images acquired using echo-planar imaging (EPI) pulse sequences, which are often employed in functional MRI (fMRI) experiments. Two EPI images with different echo times can be used to estimate the magnetic field [1], but such a field will be in a “warped” coordinate space due to the distortions in the images used for estimation. While there are correction methods for using this type of field map [1,2], it is incompatible with methods shown to provide the best correction, especially in cases of large inhomogeneity [3,4]. These require a map in “non-warped” or true coordinate space, which is usually acquired with gradient-recalled echo (GRE) images. Through an iterative process described below, an EPI based field map can be effectively transformed into true coordinate space, allowing the application of a more effective correction scheme. This eliminates the need for a potentially lengthy GRE image acquisition for field map estimation. Also, because the field map can be estimated in-line with the experiment as described in [1], the potential for motion between the estimation of the field and the actual experiment is minimized.

**Methods:** The iterative procedure for transforming an EPI based field map estimated from two images,  $I_1$  and  $I_2$ , acquired with  $TE_1$  and  $TE_2$  to true coordinate space is:

- (1) Perform a self-correction on the field map, i.e. correct the map with itself, using a method for EPI based field maps such as is described in [1] (our chosen method).
- (2) Correct both  $I_1$  and  $I_2$  using the result from 1 with a method utilizing a non-EPI based field map. The method used here is described in [3].
- (3) Recalculate a field map from the corrected versions of  $I_1$  and  $I_2$  from 2. When properly corrected, the calculated map should be close to zero everywhere. If the variation from zero is small, or if the change in variation from the previous iteration is small, the current iteration of the field map (result of 1) is the map in true coordinates. Otherwise, the “residual” map calculated in this step is added to the result of step 1 and this result becomes the input to 1 in the next iteration.

A simulation was used to verify the method. A theoretical magnetic field off-resonance map was generated to closely resemble an actual map estimated with experimental data (Figure 1a). A proton spin density map,  $\rho(x,y)$ , was also generated (Figure 1b). Two theoretical k-space acquisitions were simulated using:

$$S(m\Delta t) = \sum_{q=-N_x/2}^{N_x/2-1} \sum_{r=-N_y/2}^{N_y/2-1} \rho(q\Delta x, r\Delta y) \exp \left[ i\gamma\Delta t \left( \sum_{w=0}^m (G_x(w\Delta t)q\Delta x + G_y(w\Delta t)r\Delta y) + \Delta B_0(q\Delta x, r\Delta y)m \right) \right]$$

where  $N_x$  and  $N_y$  are the number of discrete points in  $\rho$  along  $x$  and  $y$ .  $G_x(t)$  and  $G_y(t)$  are readout and phase encoding gradient waveforms for a standard EPI trajectory. After acquiring  $S$ , the samples are placed in the 2D k-space matrix for image reconstruction. The values of  $m$  at which samples are acquired are not necessarily sequential and are determined by gradient sequence and other imaging parameters. Parameters for this simulation were FOV=24 cm, matrix size=96×96 ( $N_x=N_y=512$ ), and BW=125 kHz. The large  $N_x$  and  $N_y$  provide sub-voxel effects in the simulation. The first simulated image had  $TE=45$  ms, and the second had  $TE=50$  ms. No noise was added to the system to enable solid proof of concept.

**Results:** Figure 1c shows the absolute difference between the true field and the result of step 1 above in the first iteration (interpolated to 512×512 to allow direct comparison). This demonstrates that a simple “self-correction” of the EPI based map is not effective enough to recover the original magnetic field. The same difference is shown in Figure 1d after 30 iterations, demonstrating how the transformed map now closely matches the true field across the majority of the object. Some errors remain along the very edge of the object and near extremely large gradients in the field (top and bottom of the object). Figure 1e shows the “residual” field (result of step 3) for iteration 30. Most of the largest residuals correspond to areas where the field has not been completely transformed, the exception being the very top of the object. This provides reassurance of its use as a metric for transformation quality, and shows that it can be used to determine the accuracy across space. Figure 2 provides additional evidence of the usefulness of this metric. As iterations increase, the mean absolute residual field over the object is approximately indicative of the mean absolute error between the current iteration of the transformed field and the true field.

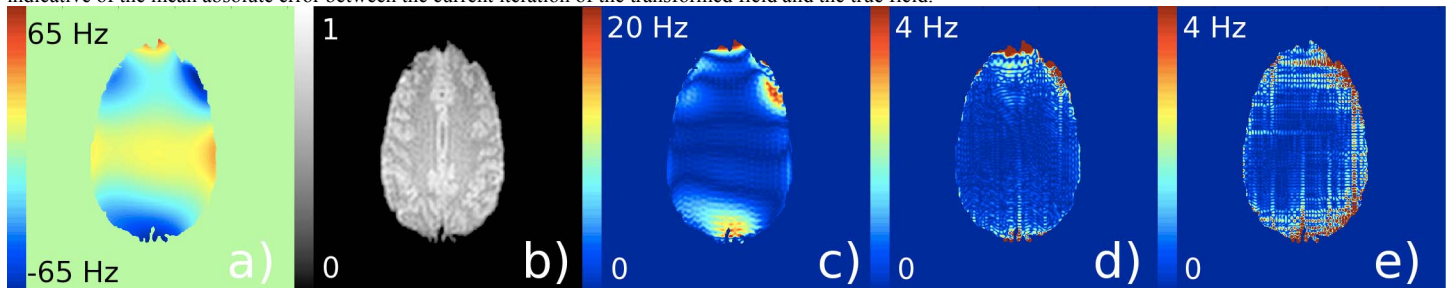
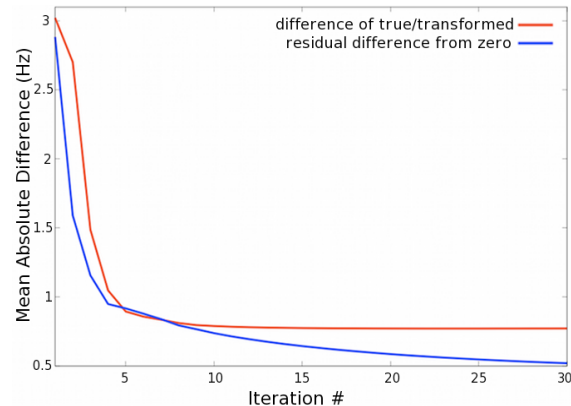


**Figure 1 (above).** (a) and (b) show maps of magnetic field off-resonance and spin density as input to the simulation respectively. (c) and (d) depict absolute error between the transformed (or unwarped) map and the true magnetic field after 1 and 30 iterations respectively. (e) shows the absolute value of the “residual” map (calculated in part 3 above) after 30 iterations.



**Discussion:** The field map used in this simulation was chosen to be an extreme case of inhomogeneity to demonstrate the limits of the method. The performance here is generally good, but demonstrates the problem presented by very large gradients in the field. It is worth noting that the same process described here was performed with the same field offset at half strength, and accuracy across the entire object within 1-2 Hz was achievable, even in the areas of strong gradient. Also important, Figure 2 also demonstrates a disconnection between the residual mean error and the true mean error as iterations increase. Performing more than 10-12 iterations provides no real value, but the residual metric continues to decrease, although both flatten out together.

**References:** 1. PJ Reber et al.: Magn Reson Med 39:328-330, 1998. 2. YM Kadah, X Hu: Magn Reson Med 38:615-627, 1997. 3. DC Noll et al.: IEEE Trans Med Imaging 10:629-637, 1991 4. P Munger et al.: IEEE Trans Med Imaging 19:681-689, 2000.

**Acknowledgements:** Funded in part by EB000215 and EB007827.

**Figure 2 (left).** Plots of mean absolute difference between the true field and the unwarped field (red) and the mean absolute residual (blue)